



Communication

Superparamagnetic Fe/Au Nanoparticles and Their Feasibility for Magnetic Hyperthermia

Mohamed F. Sanad ¹, Bianca P. Meneses-Brassea ¹, Dawn S. Blazer ¹, Shirin Pourmiri ², George C. Hadjipanayis ² and Ahmed A. El-Gendy ¹,*

- Department of Physics, University of Texas at El Paso, El Paso, TX 79968, USA; mfsanad@miners.utep.edu (M.F.S.); bmenesesbr@miners.utep.edu (B.P.M.-B.); dsblazer@miners.utep.edu (D.S.B.)
- Department of Physics and Astronomy, University of Delaware, Newark, DE 19716, USA; pourmiri@udel.edu (S.P.); hadji@udel.edu (G.C.H.)
- * Correspondence: aelgendy@utep.edu

Abstract: Today, magnetic hyperthermia constitutes a complementary way to cancer treatment. This article reports a promising aspect of magnetic hyperthermia addressing superparamagnetic and highly Fe/Au core-shell nanoparticles. Those nanoparticles were prepared using a wet chemical approach at room temperature. We found that the as-synthesized core shells assembled with spherical morphology, including face-centered-cubic Fe cores coated and Au shells. The high-resolution transmission microscope images (HRTEM) revealed the formation of Fe/Au core/shell nanoparticles. The magnetic properties of the samples showed hysteresis loops with coercivity (HC) close to zero, revealing superparamagnetic-like behavior at room temperature. The saturation magnetization (MS) has the value of 165 emu/g for the as-synthesized sample with a Fe:Au ratio of 2:1. We also studied the feasibility of those core-shell particles for magnetic hyperthermia using different frequencies and different applied alternating magnetic fields. The Fe/Au core-shell nanoparticles achieved a specific absorption rate of 50 W/g under applied alternating magnetic field with amplitude 400 Oe and 304 kHz frequency. Based on our findings, the samples can be used as a promising candidate for magnetic hyperthermia for cancer therapy.

Keywords: Fe/Au nanoparticles; superparamagnetic; core/shell; magnetic nanoparticle hyperthermia



Citation: Sanad, M.F.;
Meneses-Brassea, B.P.; Blazer, D.S.;
Pourmiri, S.; Hadjipanayis, G.C.;
El-Gendy, A.A. Superparamagnetic
Fe/Au Nanoparticles and Their
Feasibility for Magnetic
Hyperthermia. *Appl. Sci.* 2021, 11,
6637. https://doi.org/
10.3390/app11146637

Academic Editor: Andrea Atrei

Received: 28 June 2021 Accepted: 17 July 2021 Published: 20 July 2021

Publisher's Note: MDPI stays neutral with regard to jurisdictional claims in published maps and institutional affiliations.



Copyright: © 2021 by the authors. Licensee MDPI, Basel, Switzerland. This article is an open access article distributed under the terms and conditions of the Creative Commons Attribution (CC BY) license (https://creativecommons.org/licenses/by/4.0/).

1. Introduction

Magnetic nanoparticle hyperthermia (MNH) treatment is a preferable systematic strategy for cancer therapy compared to radio- or chemotherapy due to its minimized side effects on normal tissues [1–5]. Magnetic nanoparticles can be localized in deep tissues, where alternating magnetic field can move them and lead to heating power which can be used for hyperthermia applications in cancer therapy. The magnetic hyperthermia therapy is based on the fact of the tumor response to heat more than the normal cells and by increasing the temperature of body tissue to more than 42 °C yields selective damage of cancer cells and renders them more sensitive to radiation and anticancer drugs. The feasibility of such magnetic nanoparticle hyperthermia has been obtained using heat mediators of superparamagnetic nanoparticles [1–5]. However, it requires a high modality for the treatment of different cancers using the dissipated heating power known as specific absorption rate (SAR). SAR is caused by the excessive oscillations (Neel and Brownian relaxations) of the superparamagnetic nanoparticles which induced by the controllable alternating magnetic field and frequency [6–8]. Here, magnetic particles are introduced into the tumor tissue and exposed to external AC magnetic fields to increase the tumor temperature above 42 °C. Consequently, large power losses (SAR) of the magnetic nanoparticles are desirable in order to reduce the amount of material to be applied to a patient. Recently, many attempts have been made to develop a large number of biocompatible superparamagnetic nanoparticles

Appl. Sci. **2021**, 11, 6637

such as ferrites (MFe₂O₄ where M=Fe, Mn, Co, Ni, Zn) that have a large spectrum of magnetic characteristics [9–12]. Multifunctional nanocomposite surfaces can be used like a bio-functional stage for drug delivery [13,14]. Recent reports showed that to cause direct cellular death in tumors, the induced heating power under therapeutic magnetic field and frequency should produce localized heating up to 50 °C [5,15]. The generated heating power and the efficiency of the magnetic hyperthermia treatment depend on some factors, including particle size, magnetic susceptibility, and particle dispersion in the biomedical medium. These parameters need to be optimized before the in vitro/in vivo and preclinical studies. Many trials were performed to optimize some or all of those factors using different methods of particle preparations [16,17]. Other work has been developed to enhance the particles dispersion and biocompatibility in biological solutions using thermal seed of alloys, iron oxides as colloidal mediators, and Ni-Cu nanoparticles [17–23]. Although there have been many works to optimize the heating power-related factors, nanoparticles still represent considerable technical challenges like the formation of clusters and agglomerates, which negatively affect the total output heating power [24,25]. Core/shell nanospheres seem to be a promising material that can solve all the previously mentioned heating powerrelated challenges [26–31]. It is important to cover the sureface of the metallic nanparticle to avoid aire oxidation and to maintain high magnetization. Plasmonic metals such as gold and silver can be ideal shell for the nanoarpticles because of its biocompatibility, low reactivity and chemical stability.

Our hypothesis assumes that iron/gold (Fe/Au) core/shells can be a good candidate for magnetic hyperthermia direction. This is because of the high magnetic characteristics of iron, which can produce an efficient heating power to kill cancer cells, and the stability of the Au shells, which protect the Fe from further oxidation. In addition, Au shell can reduce the magnetic particle-particle interactions between Fe particles leading to better dispersion in the biological solutions (Figure 1a). Iron gold core shells were successfully designed using wet chemical methods in previous reports with a high ratio of iron oxides impurities, which hinder the magnetic capabilities of the material and some of them reported their ability for photothermal hyperthermia [32–34]. Here, we used the same wet chemical method with more controlled precautions to design pure Fe metal coated with Au nanoparticles. Material synthesis had been carried out under vigorous controlled conditions by in-situ reduction of iron prescuros and by avoiding any air exposure. The morphology, crystal structure and magnetic properties of the samples have been characterized using scanning electron microscopy (SEM), transmission electron microscopy (TEM), X-ray diffractometry (XRD), vibrating sample magnetometry (VSM), and magnetic hyperthermia, respectively. The as prepared iron gold core shell samples achieved magnetic hyperthermia performance better than recently reported work [31–33].

Appl. Sci. 2021, 11, 6637 3 of 9

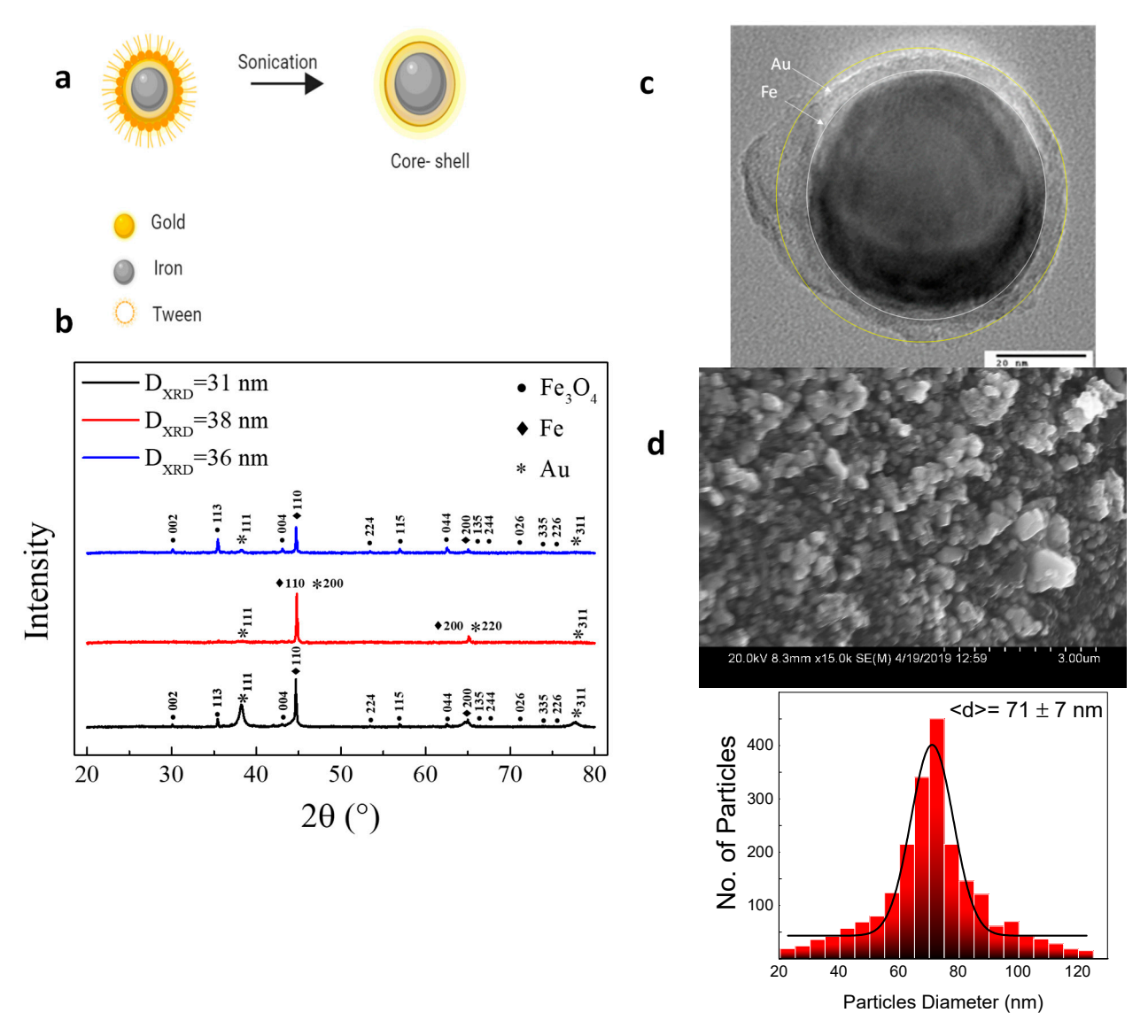


Figure 1. (a) The schematic diagram represents Fe/Au core/shell synthesis, (b) XRD patterns of Fe/Au core-shell nanoparticles with different metal ratios 1:1, 2:1, and 3:2; (c) HR-TEM of the Fe/Au core-shell assembly; (d) size distribution of the as-prepared Fe/Au core-shell nanoparticles.

2. Materials and Methods

2.1. Materials

Potassium ferricyanide, gold chloride, iron chloride, sodium borohydride, absolute ethanol, and tween were purchased in a highly pure form from Fisher Scientific, LLC (Pittsburgh, PA, USA).

2.2. Fe/Au Core/Shell Material Synthesis

Potassium ferricyanide reduction reactions were conducted in ethanol. In a typical synthesis, ferricyanide (2 mmol) was dissolved in absolute ethanol to form a yellow solution. Sodium borohydride (NaBH4) was then added to reduce the potassium ferricyanide to iron nanoparticles (Solution A). HAuCl4 (dehydrated, 0.7 mmol) was dissolved in ethanol (Solution B). Solution A was added into Solution B rapidly with continuous stirring at room temperature. The number of moles of all reagents used in the synthesis are listed in Table 1.

Appl. Sci. **2021**, 11, 6637 4 of 9

Table 1.	Used re	eagent's	concentrations.
----------	---------	----------	-----------------

	Reagents	Concentration
1	Ethanol	absolute
2	Tween	2 mL (1 M)
3	Potassium ferricyanide	2 mmol
4	Gold chloride	0.7 mmol

The color of the mixture changed to brown immediately. The mixture was further stirred for two hours and then centrifuged to remove the extra sodium borohydride. Then a 2 mL of capping agent, tween, was added into the solution followed by stirring for three hours. The sample was dried in a vacuum and washed with DI water and EtOH several times until a colorless suspension was made. A further purification stage included a magnetic separation to get separate Fe@Au from pure gold nanoparticles. The magnetically separated powder was then dried in the air, as shown in Figure 1a.

2.3. Material Characterization and Methodology

The crystal structure of Fe/Au core/shell particles was studied by X-ray diffraction [P-Analytical X′PERT MPD instrument]. Particle morphology was studied by scanning electron microscopy [FESEM JEOL6340 electron microscope] and transmission electron microscopy [H.RTEM] [JEOL-JEM-1230]. Vibrating sample magnetometry (V.S.M.) (Quantum Design, 3T Versalab) was used to study the magnetic properties. Feasibility for hyperthermia of 5 mg Fe/Au nanoparticles dispersed in 1 mL of water was measured using G2-D5 Series Multi-mode 1500W Driver from Nanoscale Biomagnetics. The sample solution was placed into the G2-D5 coil, where the alternating magnetic field amplitude and frequency can be applied. The induced temperature of the solution was detected and recorded using a fiber-optic sensor.

3. Results

The crystal structures of the synthesized Fe/Au samples have been characterized using XRD, as shown in Figure 1b. The majority of X-ray patterns show a face centered cubic (fcc structure for Fe and Au (Ref. J.C.P.D.S. 4-784) with the presence of magnetite (Fe₃O₄) peaks as a minor phase. The Rietveld refinement of the corresponding powder diffraction pattern was performed, and it was found that 31 wt% Fe, 17 wt% Au and 52 wt% magnetite were present in samples prepared at 1:1 Fe:Au ratio, and 38 wt% Fe, 41 wt% Au and 21 wt% magnetite in the sample prepared at 3:2 Fe:Au ratio. However, for the sample prepared at a 2:1 ratio, the XRD peaks confirmed the formation of pure bcc Fe coated with Au with 78 wt% Fe and 22 wt% Au. The crystalline size of the samples was calculated using the Scherer equation revealing crystalline sizes of 31, 38, 36 nm for all samples synthesized at Fe:Au precursor's ratio of 1:1, 2:1, and 3:2, respectively. To investigate the morphology and the size distribution of the produced nanoparticles, highresolution transmission electron microscopy (HRTEM) and scanning electron microscopy (SEM) have been used, respectively. Figure 1c,d shows HRTEM image and size distribution determined from SEM images of the prepared Fe/Au core/shell nanoparticles. HRTEM image displays the formation of spherical-like shape and shows the construction of the core/shell of the Fe/Au nanoparticles (Figure 1c). Note that the Fe/Au system is magnetic which reduces the resolution of the images. The size distribution was determined from the scanning electron microscope images that show homogenous distribution of the particles with average size close to 71 \pm 15 for the 2:1 Fe:Au sample (Figure 1d). The size distribution for the other 1:1 and 3:2 Fe:Au ratios averages 61 ± 21 and 83 ± 22 respectively. The field dependence of magnetization (hysteresis loops) of the samples has been measured at 300 K, as shown in Figure 2. The samples show hysteresis loops with nearly zero coercivity (Hc), revealing superparamagnetic-like behavior at room temperature. The results yield high values of saturation magnetization (M_s) of 79, 165, 89 emu/g for samples prepared at

Appl. Sci. **2021**, 11, 6637 5 of 9

Fe:Au ratios of 1:1, 2:1, and 3:2, respectively. The sample of 2:1 Fe:Au ratio show high magnetization of 165 emu/g which proves the formation of pure Fe core in the sample and in good agreement with XRD data that revealed pure Fe for the 2:1 sample. Since the size distribution is approximately the same for all samples, one can assume that the magnetization is independent of particle size. Herein, the Fe content ratio in each sample can be the reason for the observed change in magnetization values for the samples. Based on the magnetization results, the mass ratio of the magnetic core (Fe) in the Fe/Au samples can be determined by comparing their M_s value to M_s of their related bulk Fe yielding 34, 72, 39 wt% of the magnetic Fe in the 61 ± 21 , 71 ± 7 , 83 ± 21 Fe/Au samples respectively [29].

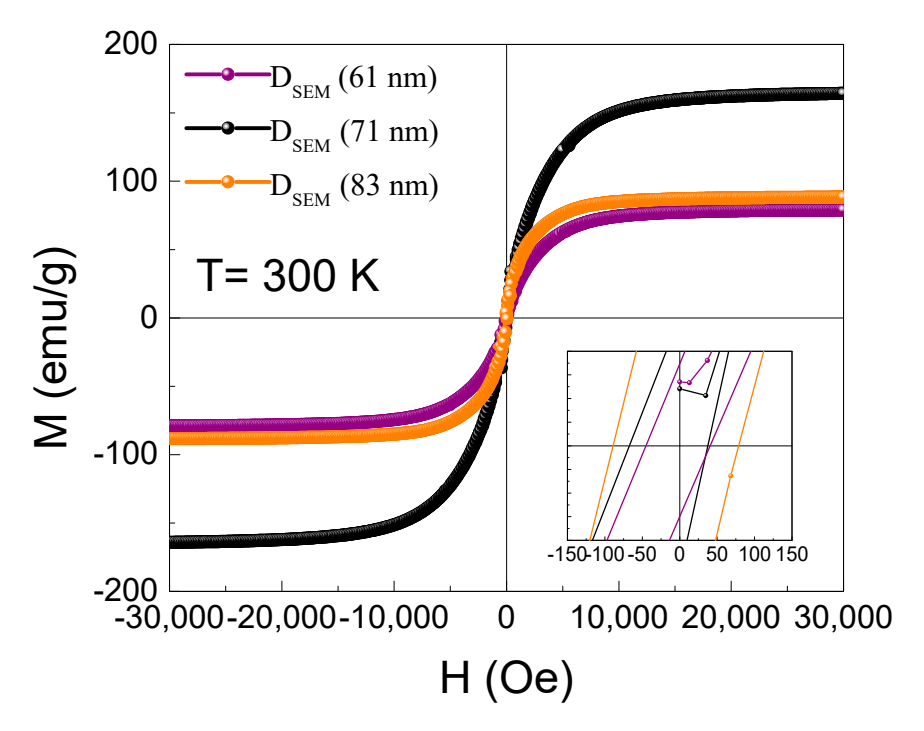


Figure 2. M-H curves at 300 K for Fe/Au core-shell nanoparticles.

The results are consistent with the phase structural data obtained from XRD and TEM The sample with a 2:1 ratio shows a high magnetization of 165 emu/g that confirms the presence of Fe core nanoparticles. In contrast, the lower magnetization of samples with 1:1 and 3:2 ratios confirms the presence of a mixture of Fe (primary phase) and Fe_3O_4 (minor phase). The presence of Fe_3O_4 nanoparticles is sufficient to reduce the net magnetization of the samples. The novelty of this work is that the magnetization of our samples is higher than all the previous trials made in this system [31–34]. In addition, comparison of coercivity and saturation magnetization with literatures is shown in Table S1.

To describe the feasibility of the prepared Fe/Au nanoparticles for magnetically induced heating, in contrast to the measurements presented above, the following experiments have been performed by means of dispersed particles in an aqueous solution. The dispersions have been prepared using distilled water as a biocompatible environment that is similar to the human biological body. The particles were dispersed in a water solution using a sonicator and vortex shaker with particles concentration of 5 mg/mL. The heating effect of the dispersed particles solution in alternating magnetic fields was studied by means of a high frequency generator with water-cooled magnetic coil system. Alternating magnetic fields with a frequency range of 144-304 kHz and magnetic field strengths of 0-500 Oe were applied to the samples. The temperature of the sample was measured by a fiber-optical temperature sensor. The solution temperature versus the exposure time (Txt) was detected and recorded using a fiber-optic sensor, as shown in Figure 3. It presents time-dependent calorimetric measurements at different applied magnetic fields for all the prepared samples. A significant heating effect is observed at applied magnetic fields for

Appl. Sci. 2021, 11, 6637 6 of 9

both samples for both samples more prominent than 200 Oe. At the maximum applied magnetic field and frequency of 400 Oe and 304 kHz, the heating rate reached values of 4 °C/min for a sample of 2:1 Fe:Au ratio and size of 71 nm. The heating effect of the other Fe:Au ratios are lower than of 2:1 balance. Based on the obtained data we cannot judge whether this is due to the agglomeration of 1:1 and 3:2 Fe:Au ratios to larger magnetic agglomerates in the suspension or caused by the less amount Fe particles and a large amount of magnetite in those ratios, which result in lower magnetization and hence reduce the induced heating power by the particles.

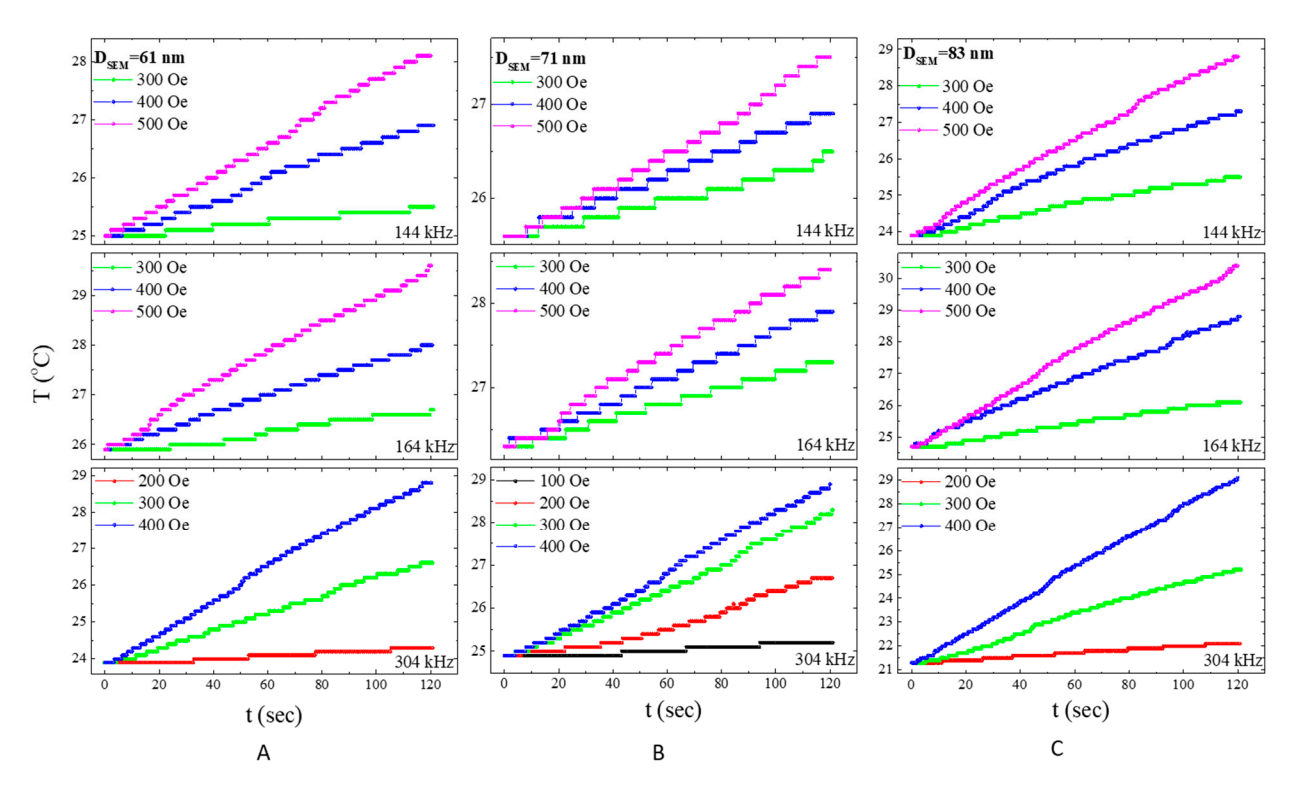


Figure 3. Temperature vs. time at different fields and frequencies for samples with sizes of (A) 61 nm, (B) 71 nm, (C) 83 nm.

It is clear that when the applied magnetic field and frequency increase, faster rotation of the magnetic moment and nanoparticles itself are obtained in the solution releasing an expansion of the temperature of the sample. The induced heating power of the magnetic nanoparticles under applied alternating magnetic fields is usually described in terms of the specific absorption rate (SAR). The SAR expresses the heating ability of the magnetic nanoparticles and, therefore, their feasibility for application in magnetic hyperthermia for cancer treatment. The induced heating power per unit mass of the sample (SAR), was calculated from the initial slope of temperature versus time plots (Figure 4) using the following equation:

$$SAR = \frac{C_p}{m_{act}} \left(\frac{dT}{dt}\right)_{t=0} \tag{1}$$

where C_p is the water-specific heat $(4.18 \,\mathrm{J \cdot g^{-1} \cdot K^{-1}})$, $m_{\rm act}$ is the mass of the sample over the total mass (in our case, the total mass = sample mass + 1 mL solution of distilled water) and $(dT/dt)_{t=0}$ is the initial slope of temperature-time data obtained from the magnetic hyperthermia experiment [7]. Figure 4 shows the heating rate and specific absorption rate SAR. on the magnetic field strength for each frequency for the prepared three samples. The 2:1 Fe:Au sample with higher Ms is producing a maximum heating rate up to 4 °C/min (Figure 4A) and SAR up to 50 W/g (Figure 4B) under therapeutic magnetic field intensities and frequencies. The observed quadratic field dependence is in agreement with the fact that the dissipated heating power is proportional to H². Heating of magnetic nanoparticles in an

Appl. Sci. **2021**, 11, 6637 7 of 9

alternating magnetic field may be understood in terms of several types of energetic barriers which must be overcome for reversal of the magnetic moments [6]. With decreasing particle size, these barriers decrease and the probability of jumps of the spontaneous magnetization due to the thermal activation processes increases, i.e., superparamagnetism evolves. Hence different heating mechanisms might appear concomitantly from which Ne'el and Brownian relaxation are expected to be the relevant processes for the observed power absorption [6]. The obtained results are considered unique for the Fe/Au system that has no recorded hyperthermia work before due to the difficulty of preparing such system with high magnetic properties. Therefore, the results open new routes to use the potential of Fe/Au nanoparticles for future in-vitro/in-vivo application in hyperthermia treatment of cancer.

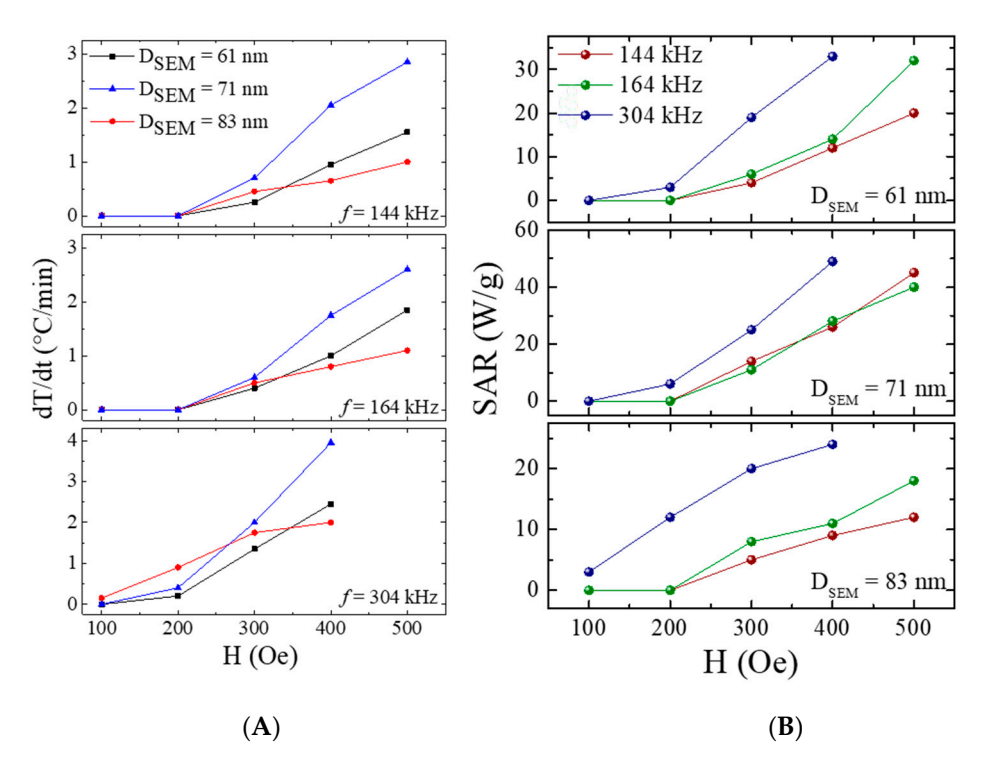


Figure 4. The effect of changing applied A.C. magnetic fields (H) at different frequencies *f* for samples with morphological sizes 61, 71, 83 nm on (**A**) the temperature and (**B**) S.A.R.

4. Conclusions

Fe/Au core/shell nanoparticles have been successfully synthesized using a wet chemistry method at ambient conditions and have been investigated with respect to their structural and magnetic properties. Our SEM and TEM studies show that gold coated nanoparticles with Fe core are formed (a core/shell structure) with a size distribution from few tens nanometers. The as-prepared nanoparticles show Fe/Au with a spherical-shape and an average size of 71 nm. X-ray diffraction was applied to confirm the phase of the core material. The size of the core particles has been deduced from the width of the XRD peaks. XRD patterns confirm the formation of pure Fe core for the 2:1 Fe:Au sample and mixture of Fe and magnetite core for the other 1:1 and 3:2 Fe:Au samples. The magnetic properties revealed superparamagnetic-like behavior for the 2:1 Fe:Au sample with high saturation magnetization at room temperature and mixture of superparamagnetic and ferromagnetic behaviors for the other 1:1 and 3:2 Fe:Au ratios. The feasibility of hyperthermia was measured for the dispersed nanoparticles in water solution, yielding good heating power showing the potential of the Fe/Au nanoparticles for hyperthermia treatment of cancer. To be specific, the samples were dispersed in water with concentration of 5 mg/mL and the heating power was recorded under applied magnetic fields and frequencies. SAR values were measured at the therapeutic range of 400 Oe and 304 kHz to yield 35, 50, 25 W/g for

Appl. Sci. **2021**, 11, 6637

synthesized samples at Fe:Au precursor's ratio of 1:1, 2:1, 3:2, respectively. The study open new route for using Fe/Au nanoparticles as a good inducing heat mediator for invitro and invivo magnetic nanoparticle hyperthermia studies for cancer treatment in the future.

Supplementary Materials: The following are available online at https://www.mdpi.com/article/10.3 390/app11146637/s1, Table S1: Comparison of coercivity and saturation magnetization with literatures.

Author Contributions: M.F.S. performed the synthesis experiments under the supervision and guidance of A.A.E.-G. and wrote the synthesis part of the manuscript. B.P.M.-B. did the characterization measurements including XRD, SEM, VSM, and hyperthermia and wrote the hyperthermia part. D.S.B. helped M.F.S. and B.P.M.-B. in the characterization analysis and writing of the manuscript. S.P. and G.C.H. have performed the TEM analysis and revised the manuscript. A.A.E.-G. designed the idea, supervised, discussed the results with the co-authors, revised and edited the manuscript. All authors have read and agreed to the published version of the manuscript.

Funding: This research was funded by US-National Science Foundation, grant number 2009358 and by National Institutes of Health, grant number RL5GM118969, TL4GM118971, and UL1GM118970.

Institutional Review Board Statement: Not applicable.

Informed Consent Statement: Not applicable.

Data Availability Statement: Not applicable.

Acknowledgments: A.A.E.-G. acknowledges the startup and rising stars funds by U.T.E.P. and UT-system, respectively.

Conflicts of Interest: The authors declare no conflict of interest.

References

- Vilas-Boas, V.; Espiña, B.; Kolen'ko, Y.V.; Bañobre-López, M.; Brito, M.; Martins, V.; Duarte, J.A.; Petrovykh, D.Y.; Freitas, P.; Carvalho, F. Effectiveness and Safety of a Nontargeted Boost for a CXCR4-Targeted Magnetic Hyperthermia Treatment of Cancer Cells. ACS Omega 2019, 4, 1931–1940. [CrossRef]
- 2. Tian, Z.; Yu, X.; Ruan, Z.; Zhu, M.; Zhu, Y.; Hanagata, N. Magnetic mesoporous silica nanoparticles coated with thermo-responsive copolymer for potential chemo- and magnetic hyperthermia therapy. *Microporous Mesoporous Mater.* **2018**, 256, 1–9. [CrossRef]
- Kandasamy, G.; Sudame, A.; Luthra, T.; Saini, K.; Maity, D. Functionalized Hydrophilic Superparamagnetic Iron Oxide Nanoparticles for Magnetic Fluid Hyperthermia Application in Liver Cancer Treatment. ACS Omega 2018, 3, 3991–4005. [CrossRef] [PubMed]
- 4. Sangnier, A.P.; Preveral, S.; Curcio, A.; Silva, A.K.A.; Lefevre, C.; Pignol, D.; Lalatonne, Y.; Wilhelm, C. Targeted thermal therapy with genetically engineered magnetite magnetosomes@RGD: Photothermia is far more efficient than magnetic hyperthermia. *J. Control. Release* 2018, 279, 271–281. [CrossRef] [PubMed]
- 5. Herea, D.-D.; Danceanu, C.; Radu, E.; Labusca, L.; Lupu, N.; Chiriac, H. Comparative effects of magnetic and water-based hyperthermia treatments on human osteosarcoma cells. *Int. J. Nanomed.* **2018**, *13*, 5743–5751. [CrossRef] [PubMed]
- 6. El-Gendy, A.; Ibrahim, E.; Khavrus, V.; Krupskaya, Y.; Hampel, S.; Leonhardt, A.; Büchner, B.; Klingeler, R. The synthesis of carbon coated Fe, Co and Ni nanoparticles and an examination of their magnetic properties. *Carbon* **2009**, *47*, 2821–2828. [CrossRef]
- 7. Tejada, J.; Ziolo, R.F.; Zhang, X.X. Quantum Tunneling of Magnetization in Nanostructured Materials. *Chem. Mater.* **1996**, 8, 1784–1792. [CrossRef]
- 8. Pankhurst, Q.A.; Connolly, J.; Jones, S.K.; Dobson, J. Applications of magnetic nanoparticles in biomedicine. *J. Phys. D Appl. Phys.* **2003**, *36*, R167–R181. [CrossRef]
- 9. Fortin, J.-P.; Wilhelm, C.; Servais, J.; Ménager, C.; Bacri, J.-C.; Gazeau, F. Size-Sorted Anionic Iron Oxide Nanomagnets as Colloidal Mediators for Magnetic Hyperthermia. *J. Am. Chem. Soc.* **2007**, *129*, 2628–2635. [CrossRef]
- 10. Sharifi, I.; Shokrollahi, H.; Amiri, S. Ferrite-based magnetic nanofluids used in hyperthermia applications. *J. Magn. Magn. Mater.* **2012**, 324, 903–915. [CrossRef]
- 11. Mazario, E.; Menendez, N.; Herrasti, P.; Cañete, M.; Connord, V.; Carrey, J. Magnetic Hyperthermia Properties of Electrosynthesized Cobalt Ferrite Nanoparticles. *J. Phys. Chem. C* **2013**, *117*, 11405–11411. [CrossRef]
- 12. Habib, A.H.; Ondeck, C.L.; Chaudhary, P.; Bockstaller, M.R.; McHenry, M.E. Evaluation of iron-cobalt/ferrite core-shell nanoparticles for cancer thermotherapy. *J. Appl. Phys.* **2008**, *103*, 07A307. [CrossRef]
- 13. Makharza, S.A.; Cirillo, G.; Vittorio, O.; Valli, E.; Voli, F.; Farfalla, A.; Curcio, M.; Iemma, F.; Nicoletta, F.P.; El-Gendy, A.A.; et al. Magnetic Graphene Oxide Nanocarrier for Targeted Delivery of Cisplatin: A Perspective for Glioblastoma Treatment. *Pharmaceuticals* **2019**, *12*, *76*. [CrossRef] [PubMed]
- 14. Kumar, C.S.; Mohammad, F. Magnetic nanomaterials for hyperthermia-based therapy and controlled drug delivery. *Adv. Drug Deliv. Rev.* **2011**, *63*, 789–808. [CrossRef]

Appl. Sci. **2021**, 11, 6637

15. Katifelis, H.; Lyberopoulou, A.; Vityuk, N.; Grammatikaki, M.; Pylypchuk, I.; Lazaris, F.; Storozhuk, L.; Kouloulias, V.; Gazouli, M. In vitro effect of hyperthermic Ag and Au Fe3O4 nanoparticles in cancer cells. *Beilstein Arch.* **2019**, 2019, 101.

- 16. Chang, D.; Lim, M.; Goos, J.; Qiao, R.; Ng, Y.Y.; Mansfeld, F.M.; Jackson, M.; Davis, T.P.; Kavallaris, M. Biologically Targeted Magnetic Hyperthermia: Potential and Limitations. *Front. Pharmacol.* **2018**, *9*, 831. [CrossRef]
- 17. Kobayashi, T.; Ito, A.; Honda, H. Magnetic Nanoparticle-Mediated Hyperthermia and Induction of Anti-Tumor Immune Responses. In *Hyperthermic Oncology from Bench to Bedside*; Kokura, S., Yoshikawa, T., Ohnishi, T., Eds.; Springer: Singapore, 2016; pp. 137–150. [CrossRef]
- 18. El-Sayed, A.H.; Aly, A.A.; Ei-Sayed, N.I.; Mekawy, M.M.; Ei-Gendy, A.A. Calculation of heating power generated from ferromagnetic thermal seed (PdCo-PdNi-CuNi) alloys used as interstitial hyperthermia implants. *J. Mater. Sci. Mater. Med.* 2007, 18, 523–528. [CrossRef] [PubMed]
- 19. Araújo-Barbosa, S.; Morales, M.A. Nanoparticles of Ni1–xCux alloys for enhanced heating in magnetic hyperthermia. *J. Alloys Compd.* **2019**, 787, 935–943. [CrossRef]
- 20. Kandasamy, G.; Sudame, A.; Bhati, P.; Chakrabarty, A.; Kale, S.N.; Maity, D. Systematic magnetic fluid hyperthermia studies of carboxyl functionalized hydrophilic superparamagnetic iron oxide nanoparticles based ferrofluids. *J. Colloid Interface Sci.* 2018, 514, 534–543. [CrossRef]
- 21. Brero, F.; Albino, M.; Antoccia, A.; Arosio, P.; Avolio, M.; Berardinelli, F.; Bettega, D.; Calzolari, P.; Ciocca, M.; Corti, M.; et al. Hadron Therapy, Magnetic Nanoparticles and Hyperthermia: A Promising Combined Tool for Pancreatic Cancer Treatment. *Nanomaterials* **2020**, *10*, 1919. [CrossRef] [PubMed]
- 22. Meneses-Brassea, B.P.; Borrego, E.A.; Blazer, D.S.; Sanad, M.F.; Pourmiri, S.; Gutierrez, D.A.; Varela-Ramirez, A.; Hadjipanayis, G.C.; El-Gendy, A.A. Ni-Cu Nanoparticles and Their Feasibility for Magnetic Hyperthermia. *Nanomaterials* **2020**, *10*, 1988. [CrossRef]
- 23. Salem, N.F.; Abouelkheir, S.S.; Yousif, A.M.; Meneses-Brassea, B.P.; Sabry, S.A.; Ghozlan, H.A.; El-Gendy, A. Large scale production of superparamagnetic iron oxide nanoparticles by the haloarchaeon Halobiforma sp. N1 and their potential in localized hyperthermia cancer therapy. *Nanotechnology* **2021**, *32*, 09LT01. [CrossRef]
- 24. Pon-On, W.; Tithito, T.; Maneeprakorn, W.; Phenrat, T.; Tang, I.M. Investigation of magnetic silica with thermoresponsive chitosan coating for drug controlled release and magnetic hyperthermia application. *Mater. Sci. Eng. C* **2019**, *97*, 23–30. [CrossRef] [PubMed]
- 25. Albarqi, H.A.; Wong, L.H.; Schumann, C.; Sabei, F.Y.; Korzun, T.; Li, X.; Hansen, M.N.; Dhagat, P.; Moses, A.S.; Taratula, O.; et al. Biocompatible Nanoclusters with High Heating Efficiency for Systemically Delivered Magnetic Hyperthermia. *ACS Nano* **2019**, 13, 6383–6395. [CrossRef] [PubMed]
- 26. Chen, X.; Klingeler, R.; Kath, M.; ElGendy, A.; Cendrowski, K.; Kalenczuk, R.; Borowiak-Palen, E. Magnetic Silica Nanotubes: Synthesis, Drug Release, and Feasibility for Magnetic Hyperthermia. *ACS Appl. Mater. Interfaces* **2012**, *4*, 2303–2309. [CrossRef] [PubMed]
- 27. Mendes, R.G.; Koch, B.; Bachmatiuk, A.; ElGendy, A.; Krupskaya, Y.; Springer, A.; Klingeler, R.; Schmidt, O.G.; Büchner, B.; Sánchez, S.; et al. Synthesis and toxicity characterization of carbon coated iron oxide nanoparticles with highly defined size distributions. *Biochim. Biophys. Acta (BBA)-Gen. Subj.* 2014, 1840, 160–169. [CrossRef]
- 28. Ibrahim, E.; Hampel, S.; Wolter, A.U.B.; Kath, M.; El-Gendy, A.A.; Klingeler, R.; Täschner, C.; Khavrus, V.O.; Gemming, T.; Leonhardt, A.; et al. Superparamagnetic FeCo and FeNi Nanocomposites Dispersed in Submicrometer-Sized C Spheres. *J. Phys. Chem. C* 2012, 116, 22509–22517. [CrossRef]
- 29. ElGendy, A.; Khavrus, V.; Hampel, S.; Leonhardt, A.; Büchner, B.; Klingeler, R. Morphology, Structural Control, and Magnetic Properties of Carbon-Coated Nanoscaled NiRu Alloys. *J. Phys. Chem. C* **2010**, *114*, 10745–10749. [CrossRef]
- 30. Mendes, R.G.; Bachmatiuk, A.; El-Gendy, A.A.; Melkhanova, S.; Klingeler, R.; Büchner, B.; Rümmeli, M.H. A Facile Route to Coat Iron Oxide Nanoparticles with Few-Layer Graphene. *J. Phys. Chem. C* **2012**, *116*, 23749–23756. [CrossRef]
- 31. Lin, J.; Zhoub, W.; Kumbhar, A.; Wiemann, J.; Fangb, J.; Carpenter, E.; O'Connor, C. Gold-Coated Iron (Fe@Au) Nanoparticles: Synthesis, Characterization, and Magnetic Field-Induced Self-Assembly. *J. Solid State Chem.* **2001**, *159*, 26–31. [CrossRef]
- 32. Ban, Z.; Barnakov, Y.A.; Li, F.; Golub, V.O.; O'Connor, C.J. The synthesis of core–shell iron@gold nanoparticles and their characterization. *J. Mater. Chem.* 2005, 15, 4660–4662. [CrossRef]
- 33. Li, Y.; Dhawan, U.; Wang, H.Y.; Liu, X.; Ku, H.H.; Tsai, M.T.; Chung, R.J. Theranostic Iron@Gold Core–Shell Nanoparticles for Simultaneous Hyperthermia-Chemotherapy upon Photo Stimulation. *Part. Part. Syst. Charact.* **2019**, *36*, 1800419. [CrossRef]
- 34. Caro, C.; Gámez, F.; Quaresma, P.; Páez-Muñoz, J.; Domínguez, A.; Pearson, J.; Leal, M.P.; Beltrán, A.; Fernandez-Afonso, Y.; De la Fuente, J.; et al. Fe₃O₄-Au Core-Shell Nanoparticles as a Multimodal Platform for In Vivo Imaging and Focused Photothermal Therapy. *Pharmaceutics* **2021**, *13*, 416. [CrossRef] [PubMed]